

Segregation of Micron-Scale Membrane Sub-Domains in Live Murine Sperm

VIMAL SELVARAJ,¹ ATSUSHI ASANO,¹ DANIELLE E. BUTTKE,¹ JOHN L. McELWEE,¹
 JACQUELYN L. NELSON,¹ COLLIN A. WOLFF,¹ TANYA MERDIUSHEV,² MIGUEL W. FORNÉS,³
 ALEX W. COHEN,⁴ MICHAEL P. LISANTI,⁴ GEORGE H. ROTHBLAT,⁵
 GREGORY S. KOPF,⁶ AND ALEXANDER J. TRAVIS^{1*}

¹The James A. Baker Institute for Animal Health, College of Veterinary Medicine,
 Cornell University, Ithaca, New York

²Center for Research on Reproduction and Women's Health,
 University of Pennsylvania Medical Center, Philadelphia, Pennsylvania

³Instituto de Histología y Embriología, Universidad Nacional de Cuyo,
 Mendoza, Argentina

⁴Department of Molecular Pharmacology, Albert Einstein College of Medicine,
 Bronx, New York

⁵Children's Hospital of Philadelphia, Philadelphia, Pennsylvania

⁶Women's Health Research Institute, Wyeth Research, Collegeville, Pennsylvania

Lipid rafts, membrane sub-domains enriched in sterols and sphingolipids, are controversial because demonstrations of rafts have often utilized fixed cells. We showed in living sperm that the ganglioside G_{M1} localized to a micron-scale membrane sub-domain in the plasma membrane overlying the acrosome. We investigated four models proposed for membrane sub-domain maintenance. G_{M1} segregation was maintained in live sperm incubated under non-capacitating conditions, and after sterol efflux, a membrane alteration necessary for capacitation. The complete lack of G_{M1} diffusion to the post-acrosomal plasma membrane (PAPM) in live cells argued against the transient confinement zone model. However, within seconds after cessation of sperm motility, G_{M1} dramatically redistributed several microns from the acrosomal sub-domain to the post-acrosomal, non-raft sub-domain. This redistribution was not accompanied by movement of sterols, and was induced by the pentameric cholera toxin subunit B (CTB). These data argued against a lipid–lipid interaction model for sub-domain maintenance. Although impossible to rule out a lipid shell model definitively, mice lacking caveolin-1 maintained segregation of both sterols and G_{M1} , arguing against a role for lipid shells surrounding caveolin-1 in sub-domain maintenance. Scanning electron microscopy of sperm freeze-dried without fixation identified cytoskeletal structures at the sub-domain boundary. Although drugs used to disrupt actin and intermediate filaments had no effect on the segregation of G_{M1} , we found that disulfide-bonded proteins played a significant role in sub-domain segregation. Together, these data provide an example of membrane sub-domains extreme in terms of size and stability of lipid segregation, and implicate a protein-based membrane compartmentation mechanism. *J. Cell. Physiol.* 206: 636–646, 2006.

© 2005 Wiley-Liss, Inc.

Lipid rafts are regions of membrane enriched in sterols and sphingolipids as opposed to phospholipids, and have been suggested to act as foci for a wide variety of cellular functions (Simons and Toomre, 2000). Two forms of raft have been proposed: the first are small (nm scale) and highly dynamic, and the second, induced by physiological crosslinking of molecules, can be larger and more stable (Kusumi et al., 2004). Several models have been put forth to explain the formation and maintenance of such sub-domains, including lipid–lipid interactions (such as tendencies for some lipids to self-aggregate, or for the aggregation of different lipids such as sterols and gangliosides), the preferential interaction of lipids with specific membrane proteins (“lipid shells”), the slowing of molecules in “transient confinement zones,” and restricted lateral diffusion of molecules between membrane compartments due to borders of transmembrane proteins/underlying cytoskeletal elements [reviewed in (Kusumi et al., 2004)].

However, there is great controversy regarding the nature and dynamics of lipid rafts in cells; specifically, that artifacts might result from exposure of cells or membranes to detergents or crosslinking reagents/fixatives [reviewed in (Munro, 2003)]. For example, the pentameric “B” subunit of cholera toxin (CTB) is used for specific localization of the ganglioside, G_{M1} (Lauer et al.,

Abbreviations: CTB, cholera toxin subunit B; APM, acrosomal plasma membrane; PAPM, post-acrosomal plasma membrane; SAR, sub-acrosomal ring; AA, apical acrosome; ES, equatorial segment; PBS, phosphate buffered saline; 2-OHCD, 2-hydroxypropyl- β -cyclodextrin; MW, modified Whitten's medium; Fixative A, 0.004% paraformaldehyde in PBS; Fixative B, 4% PF and 0.1% glutaraldehyde with 5 mM $CaCl_2$ in PBS; PCP, pentachlorophenol; SEM, scanning electron microscopy.

Vimal Selvaraj and Atsushi Asano have contributed equally to the work.

This article contains Supplementary Material available from the authors upon request or via the Internet at <http://www.interscience.wiley.com/jpages/0021-9541/suppmat>.

Contract grant sponsor: National Institutes of Health; Contract grant numbers: K01-RR00188, R01-HD-045664, P01-HD-06274, R01-CA-98779, R01-CA-80250, T32-GM07288; Contract grant sponsor: Dual Degree Program of the Cornell University College of Veterinary Medicine; Contract grant sponsor: American Heart Association Established Investigator Award; Contract grant number: 0540113N; Contract grant sponsor: Hirschl/Weil-Caulier Career Scientist Award.

*Correspondence to: Alexander J. Travis, The James A. Baker Institute for Animal Health, College of Veterinary Medicine, Cornell University, Ithaca, NY 14853. E-mail: ajt32@cornell.edu

Received 8 June 2005; Accepted 25 July 2005

DOI: 10.1002/jcp.20504

2002), but can cause patching artifacts. It has been suggested that definitive proof of lipid rafts will require visualization in living cells (Munro, 2003).

Recent studies have attempted to address such concerns. Acyl chains on modified fluorescent proteins were shown to promote the clustering or close proximity of these constructs (Zacharias et al., 2002). Shifts in fluorescence wavelength of laurdan have suggested that living macrophages have 10–15% of their cell surface covered by liquid-ordered domains (i.e., rafts), especially cell extensions and contact points (Gaus et al., 2003). These domains are larger than the nm-scale rafts believed to exist in most cells, and suggest that lipid rafts of varying size might be organized to particular regions of cells where their biophysical properties can impart specific functionality.

Mammalian sperm are highly polarized, with distinct functions restricted to specific regions. There are three major domains in the plasma membrane (the head, the mid-piece, and the principal piece of the flagellum), with sub-domains within each of these regions, making sperm an intriguing model for the study of membrane compartmentalization [reviewed in (Travis and Kopf, 2002)]. Based on work in fixed cells, the plasma membrane of the sperm head is suggested to have two major sub-domains, distinct with regard to their functions as well as their lipid and protein compositions.

The physiological relevance of studies on sperm lipid sub-domains is great, in that for sperm to fertilize an egg, they must undergo sterol efflux from their plasma membrane during the process of capacitation, which renders them competent to fertilize an egg (Davis, 1976; Visconti et al., 1999b). The acrosomal plasma membrane (APM) of a capacitated sperm interacts with the extracellular matrix of the egg, and in response, fuses with the underlying outer acrosomal membrane, which triggers the regulated exocytotic release of the acrosomal contents (Kim and Gerton, 2003). The APM itself has at least two distinct areas within the sub-domain, one over the apical acrosome (AA) and a larger one over the equatorial segment (ES). The post-acrosomal plasma membrane (PAPM) is not involved in the initial interaction with the egg's extracellular matrix, but later fuses with the egg's plasma membrane (Clark and Koehler, 1990). In fixed sperm of a number of species, the APM is enriched in sterols, whereas the PAPM is largely devoid of sterols (Friend, 1982; Pelletier and Friend, 1983; Suzuki, 1988; Lin and Kan, 1996; Visconti et al., 1999b).

Despite the potential connections between lipid sub-domains on the sperm head and the functional requirement for sterol efflux during sperm capacitation, little mechanistic information linking these observations is available. To improve understanding of lipid dynamics in live sperm, we investigated the localization of an endogenous ganglioside, G_{M1} , on the plasma membrane of the sperm head. Our findings address the current controversy surrounding whether lipid rafts can exist in live cells, demonstrating the stable segregation of endogenous G_{M1} to the plasma membrane overlying the acrosome in live murine sperm. We also investigated the mechanism underlying this segregation and provide evidence supporting a protein-based membrane compartmentation model of lipid segregation.

MATERIALS AND METHODS

Reagents and animals

All reagents were purchased from Sigma (St. Louis, MO), unless otherwise noted. CTB (Molecular Probes, Eugene, OR)

was purchased conjugated with Alexa Fluor 488 or Alexa Fluor 647 as indicated. Male CD-1 mice were from Charles River Laboratories (Kingston, NY).

Preparation of media and incubations of sperm

A modified Whitten's medium (MW; 22 mM HEPES, 1.2 mM $MgCl_2$, 100 mM NaCl, 4.7 mM KCl, 1 mM pyruvic acid, 4.8 mM lactic acid hemi-calcium salt, pH 7.35) (Travis et al., 2001a) containing 5.5 mM glucose was used for all incubations unless otherwise indicated. 2-hydroxypropyl- β -cyclodextrin (2-OHCD; 3 mM) was supplemented as needed. 2-OHCD supports sperm capacitation and *in vitro* fertilization by functioning as a sterol acceptor, and is preferred over the more potent methyl- β -cyclodextrin (Visconti et al., 1999a). Mature sperm were collected from the cauda epididymides by a swim-out procedure as described previously (Travis et al., 2001a). All steps of washing of sperm and all incubations for experiments were performed at 37°C.

Fluorescence localization of lipids

All incubations during localization experiments were carried out under dim lighting at 37°C in a humidity chamber. Sperm (2×10^6) were incubated in 300 μ l MW. The localization of G_{M1} was visualized with CTB in live sperm or after fixation under different conditions. In both cases, cells were viewed with a Nikon Eclipse TE 2000-U microscope (Nikon, Melville, NY) equipped with a Photometrics Coolsnap HQ CCD camera (Roper Scientific, Ottobrunn, Germany), and Openlab 3.1 (Improvision, Lexington, MA) automation and imaging software. Assignments of sperm to G_{M1} localization patterns were performed in a blind fashion regarding incubation condition. To compare shifts in population tendencies, the numbers were converted to percentages prior to statistical evaluation. In all cases, ≥ 100 cells were counted for each test condition, and every sperm in a given field was counted to avoid potential bias.

For localization in live sperm, a stage-mounted incubation chamber (LiveCell, Neue Product Group, Westminster, MD) was used along with an objective heater (Bioprotechs, Butler, PA). Samples were observed using glass bottom culture dishes (MatTek Corporation, Ashland, MA) overlaid with mineral oil, or using small aliquots on slides under coverslips. Samples were incubated for 10 min with CTB (10 μ g/ml). To avoid any membrane damage, some samples were not washed, but viewed with CTB in the final medium as indicated. To study the effect of sterol efflux in live sperm, MW medium supplemented with 3 mM 2-OHCD was used and the sperm were incubated for 45 min before addition of CTB. Images of motile sperm were captured using programmed exposure intervals, and serial images were tethered into QuickTime (Apple Computers, Cupertino, CA) movies.

Alternatively, for experiments designed to quantify the relative fluorescence intensities over the APM versus the PAPM, live sperm were allowed to attach to coverslips, incubated in CTB (5 μ g/ml) for 10 min, and then washed five times with MW medium. Images of motile sperm were taken before and after changes in pattern of G_{M1} localization. Using image analysis tools in Openlab 3.1, minimum, maximum, mean, and mode fluorescence intensity per pixel (arbitrary units) were recorded for the whole sperm head and for equal-sized circles drawn within the APM and PAPM, before and after change in G_{M1} localization. Background fluorescence intensity was measured in identically sized circles immediately adjacent to the sperm head, and these values were subtracted from each measurement within the sperm head to adjust for local differences in background and for any signal quenching that might have occurred between images taken of the same cell. Means for the signal intensity over the whole sperm head, the APM, and the PAPM were compared within cells that exhibited a change in localization pattern, using the Wilcoxon-signed rank test for non-parametric data.

For localization of G_{M1} in fixed sperm, the cells were incubated in MW medium, allowed to attach to coverslips for 30 min, and then fixed for 15 min with either: (I) 0.004% paraformaldehyde (PF) in PBS [hereafter referred to as "Fixative A"], (II) 2% PF in PBS, (III) 2% PF and 1% glutaraldehyde in PBS, (IV) 1.25% PF and 2.5% glutaraldehyde in 100 mM

sodium cacodylate and 0.5 mM CaCl₂, or (V) 4% PF and 0.1% glutaraldehyde with 5 mM CaCl₂ in PBS [hereafter referred to as "Fixative B"]. The sperm were washed with PBS and incubated for 10 min with CTB (10 µg/ml). The sperm were washed again and mounted. Alternatively, sperm were fixed while in suspension, washed by centrifugation and resuspension, incubated with CTB as above, and then washed again by centrifugation and resuspension. This method was less preferred because of membrane damage. Further, to confirm that crosslinking by CTB, and not the weak fixation itself, was inducing an observed redistribution of G_{M1}, serial fixation experiments were carried out. These sperm were first fixed with Fixative A for 15 min followed by incubation with Fixative B for 15 min prior to labeling with CTB, washing, and mounting.

Filipin localization of membrane sterols

For localization of filipin-sterol complexes in sperm membranes in conjunction with G_{M1}, sperm were incubated in MW medium with glucose, allowed to attach to coverslips for 30 min, and then fixed for 15 min with either Fixative A or Fixative B. The sperm were washed with PBS and incubated for 10 min with Alexa Fluor 647 CTB (10 µg/ml), washed and then incubated with filipin complex [50 µg/ml in methanol, final concentration 0.3% (v/v)] for 10 min. Sperm were then washed and coverslips were mounted on slides with ProLong Gold Antifade (Molecular Probes). Filipin-sterol complexes were visualized at 340–380 nm excitation.

Indirect immunofluorescence

Sperm were incubated, allowed to attach to coverslips, and fixed as described above. Sperm were washed, blocked for 30 min in PBS with 1% bovine serum albumin, and then incubated with anti-G_{M1} (1:500; Matreya, Pleasant Gap, PA) for 1 h. They were then washed, incubated with secondary antibody (1:500) for 30 min, washed again, and mounted as above. A control for non-specific binding was performed with sperm incubated with secondary antibody alone.

Caveolin-1 null mice

Caveolin-1 null mice (Cav-1^{-/-}) in the C57BL/6 genetic background were generated as previously described (Razani et al., 2001). For these experiments, sperm were collected from 20-week-old homozygous Cav-1^{-/-} and corresponding wild-type cohorts (n = 2 for each) as described above. Fluorescence localization of G_{M1} using CTB on both live and fixed sperm and localization of membrane sterols using filipin complex on fixed sperm were also carried out as described above.

ATP depletion and assay

Sperm (2 × 10⁶/30 µl) were pre-incubated with 10 mM sodium azide and 0.2 mM pentachlorophenol (PCP) or DMSO (0.1% v/v; solvent control) for 10 min in MW with no glucose, pyruvate or lactate. Samples were then diluted to 2 × 10⁶ sperm/300 µl and incubated for an additional 20 min. Sperm motility was monitored under the microscope after each incubation step. Samples were then fixed with Fixative B for 15 min. Fixed sperm were processed for G_{M1} labeling using CTB as described earlier.

For quantification of ATP, sperm treated with 10-mM sodium azide and 0.2-mM PCP were incubated as above, monitored for the cessation of motility, and then used for determining sperm ATP concentration post-ATP depletion with the ENLITEN[®] ATP Assay System Bioluminescence Detection Kit according to the manufacturer's instructions (Promega, Madison, WI). One hundred milliliters of 2% TCA and 0.2% Triton were added to 50 ml of a dilution of sperm. Tubes were incubated on ice for 15 min and vortexed every 5 min. After centrifugation to remove the pellet, the supernatant was diluted again, prior to mixing with the assay reagents and quantifying luminescence. Controls included untreated cells and medium alone.

Disruption of actin and intermediate filaments

Sperm in MW medium were treated for 20 min with either 50 µM cytochalasin D, 5 µM latrunculin A, 1 µM swinholide A,

or DMSO (0.1% v/v; solvent control) to disrupt the actin cytoskeleton. Similarly, sperm were incubated in MW medium containing either 10 or 100 mM acrylamide (Bio-Rad, Hercules, CA) for 20 min to disrupt intermediate filament organization. After treatment, sperm were either incubated with CTB and viewed as live cells as above, or were fixed with Fixative B for 15 min. Fixed sperm were processed for G_{M1} labeling using CTB as described earlier. Statistical analyses for the different treatments were carried out first comparing patterns across all the groups using Kruskal–Wallis rank sum test for non-parametric data. Pairwise comparisons between treatment groups were done on arcsine-transformed data using Tukey's HSD.

Treatment with disulfide-reducing agents

Sperm were incubated in the presence of different concentrations of L-dithiothreitol (DTT) or β-mercaptoethanol (βME) for 20 min, and were either incubated with CTB and viewed as live cells as above, or were fixed with Fixative B for 15 min. The cells were then washed two times by centrifugation and resuspension to remove DTT. Sperm were then processed for G_{M1} labeling using CTB as described. Prior to fixation, sperm motility was estimated in all samples using light microscopy. To investigate the effect of DTT on sperm post-fixation, sperm fixed for 15 min with either Fixative A or Fixative B were washed by centrifugation and resuspension using PBS and then incubated with 1-mM DTT for 20 min. After treatment, sperm fixed with Fixative A were again fixed with Fixative B for 15 min. All samples were washed to remove DTT and fixatives and processed for G_{M1} labeling using CTB as described. Statistical analyses for the different treatments were carried out first comparing patterns across all the groups using Kruskal–Wallis rank sum test for non-parametric data. Pairwise comparisons between treatment groups were done on arcsine-transformed data using Tukey's HSD.

Scanning electron microscopy

SEM was performed on both unfixed, freeze-dried sperm, and on fixed sperm subjected to critical point drying. In the first method, sperm in PBS were frozen in nitrogen slush and then freeze-dried for 3 days at -42°C at 95 mT in a VirTis Freeze-mobile (VirTis, Gardiner, NY). The chip was coated with 30 nm of gold palladium in a Bal-Tec SCD 050 sputter coater (Balzers Union, Liechtenstein, Germany), and viewed with a Hitachi S4500 scanning electron microscope (Mountain View, CA). In the second method, sperm were fixed for 2 h with 2.5% glutaraldehyde in 100 mM sodium cacodylate and 1% tannic acid at pH 7.4 in a culture tube. After washing by centrifugation and resuspension, they were fixed with 2% osmium tetroxide and 2% sodium cacodylate at 4°C overnight. The cells were washed and dehydrated in ethanol with a 20 min incubation in 2% uranyl acetate at 70% ethanol. Once in absolute ethanol, they were critical point dried, coated, and viewed. Digital micrographs were collected using a Princeton Gamma Tech digital beam acquisition program (Imix, Princeton, NJ).

RESULTS

G_{M1} localization and redistribution in the sperm head

In live motile sperm, G_{M1} localized to the APM (Fig. 1A,B). The distribution of G_{M1} to the APM was uniform with a clear separation of signal from the PAPM at the level of the sub-acrosomal ring (SAR). All motile sperm in the medium had the same localization pattern. This pattern of localization was very stable and did not alter the entire time a sperm was viable and motile. CTB fluorescence was always confined to the APM and was never seen to diffuse across the SAR in live sperm. This finding argues against a transient confinement zone model of sub-domain maintenance, which would instead describe a state in which G_{M1} would diffuse more slowly over the APM, but not be excluded from the PAPM.

Importantly, this segregation of G_{M1} to the APM was maintained even after sterol efflux with 2-OHCD (3 mM)

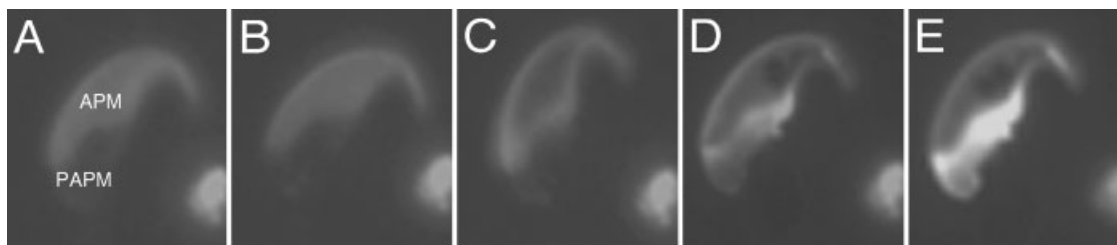


Fig. 1. Localization of G_{M1} in live sperm with CTB. Parts A–E are single exposures taken from a series of images of a live, non-capacitated sperm, showing redistribution of G_{M1} upon the cessation of motility. Parts A and B represent the pattern seen in the motile sperm, whereas parts C–E show stages in the redistribution of G_{M1} in the same cell when immotile. A movie of this redistribution is available as supplemental material (Video 1).

for 60 min (Supplemental Material, Fig. 1), a concentration and duration of incubation sufficient to induce the level of sterol efflux necessary for sperm capacitation (Visconti et al., 1999a).

However, within seconds after the cessation of motility, the pattern of CTB fluorescence changed dramatically, appearing to lessen over the APM and brightening strongly over the PAPM (Fig. 1C–E and movie in Supplemental Material, Video 1). First, the signal decreased from within the ES and increased at the borders of the APM (the AA, the SAR, and the perforatorium), prior to extending into the PAPM. The redistribution occurred within 10–100 sec after the cessation of motility. This change was consistent with the pattern seen in dead sperm and was not associated with acrosomal exocytosis (data not shown). Similar localization of G_{M1} to the PAPM was also seen in most sperm that were not motile at the beginning of these same experiments, suggesting that the loss of segregation coincided with the sperm becoming non-viable.

Two possibilities exist for the change in pattern seen upon the cessation of motility/death. The first would be a redistribution of G_{M1} from the APM to the PAPM, whereas the second would involve the unmasking or appearance of new G_{M1} on the outer leaflet of the PAPM in conjunction with some degree of redistribution. To distinguish between these possibilities, we repeated these experiments with repetitive washing out of unbound CTB from the medium. This would minimize free CTB available to bind to new molecules of G_{M1} that might become exposed in the PAPM. Quantification of fluorescence intensity in the APM against the PAPM revealed a statistically significant decrease in the APM coincident with a significant increase in signal in the PAPM (Fig. 2A,B,D). These changes, and the pattern of movement seen in Figure 1 indicate that redistribution did indeed occur.

However, the decrease in signal over the APM could not account for the disproportionate increase in fluorescence intensity over the PAPM, even taking into consideration the fact that the PAPM is approximately one-half the size of the APM (Fig. 2B,D). The increase in fluorescence associated with the PAPM also caused an increase in whole head intensity after redistribution (Fig. 2C). To determine if redistribution induced some change in the fluorescence properties of the fluorophore (Maxfield, 1982), we used both a fluorimeter and ELISA plate reader to quantify total fluorescence intensity of AlexaFluor 488-conjugated CTB in entire incubation tubes before and after the CTB-induced redistribution of G_{M1} (In separate experiments with $n \geq 3$, these readings were taken both with excess CTB in the medium, and after washing out unbound CTB. In addition, in separate experiments, sperm were allowed to lose motility on

their own, or by the addition of Fixative A.). We did not detect a significant change in total fluorescence of the system under any of these conditions (data not shown). Interestingly, experiments involving the quenching of fluorophores conjugated to CTB have suggested that internalization and reappearance of G_{M1} in the APM is also occurring prior to redistribution, suggesting that a combination of mechanisms is responsible for the change in pattern (Buttke, Selvaraj, Asano, and Travis, manuscript in preparation). We are therefore continuing to investigate this phenomenon.

Immunolocalization with anti- G_{M1} antibody

To corroborate that CTB was in fact binding to G_{M1} in the APM, we performed indirect immunofluorescence experiments with a bivalent primary antibody against G_{M1} on sperm fixed with Fixative A (Fig. 3) or with a strong fixative (Fixative B; results were identical between the two fixation conditions, data not shown). This low concentration of PF (Fixative A) was tested because it has been reported to immobilize sperm without permeabilization (Harrison and Vickers, 1990). We observed fluorescence over the APM of most sperm incubated under both non-capacitating conditions or in the presence of 2-OHCD (Fig. 3). These findings verified the segregation of G_{M1} seen in live cells with CTB.

Specific fixation conditions prevented G_{M1} redistribution

Different fixation conditions were tested to see whether the G_{M1} could be immobilized and redistribution prevented, three of which are shown in Table 1. The patterns of G_{M1} localization seen in sperm under different fixation conditions are described as “APM” for fluorescence over the APM, “D” for a diffuse fluorescence all over the sperm head, “AA/PAPM” where the AA and PAPM show fluorescence, and “PAPM” for fluorescence over the PAPM.

The weak fixative (Fixative A) caused almost all sperm to show G_{M1} redistribution with CTB, with signal over the PAPM (Table 1). Fixation with 2% PF in PBS and fixation with 2% PF and 1% glutaraldehyde could prevent CTB-induced G_{M1} redistribution in a small proportion of sperm, and results for these conditions between samples were variable (data not shown). The next fixation condition tested, 1.25% PF and 2.5% glutaraldehyde in 100 mM sodium cacodylate and 0.5 mM $CaCl_2$, immobilized G_{M1} to the APM in about 75% of sperm incubated under non-capacitating conditions (Table 1). However, this fixative was not adequate to immobilize G_{M1} in cells incubated with 2-OHCD (data not shown). Ultimately, the use of Fixative B was adequate to immobilize the lipids in 80% of the sperm regardless of the incubation condition. These data

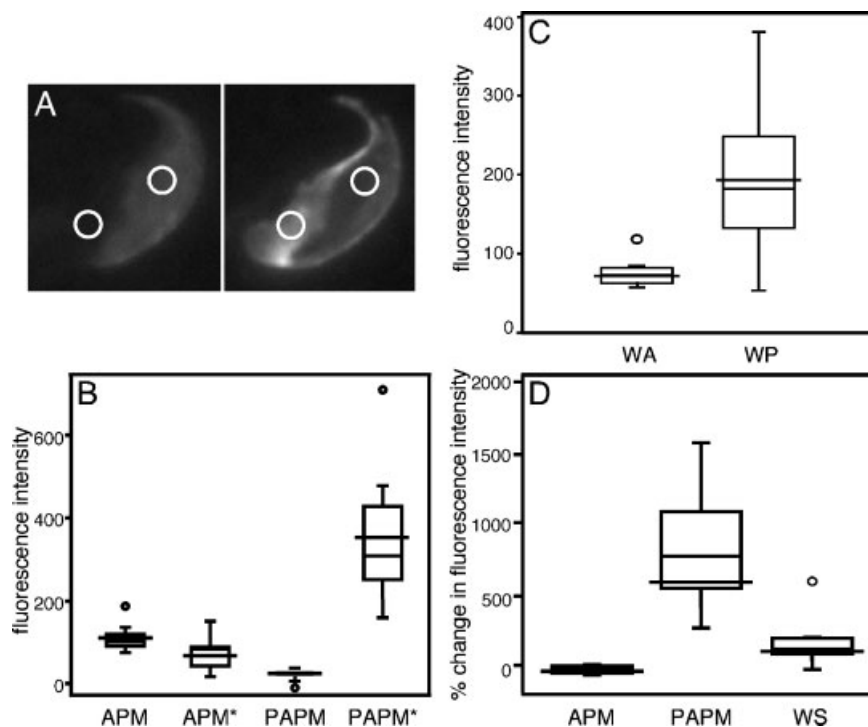


Fig. 2. Fluorescence intensity of CTB in different regions of the sperm head. Images were taken of live sperm having an APM pattern of fluorescence and then again at the same exposure settings after cessation of motility when they displayed a PAMP pattern ($n=9$). Mean fluorescence intensities within the APM and PAMP were recorded before and after (*) the shift in pattern of localization (Part B), using an equal-sized circle within each region (Part A). Fluorescence intensity was also recorded for the whole sperm head before (WA) and after (WP) the shift in localization pattern (Part C). Results are shown as box-whisker plots in Parts B–D, with the boundaries of the boxes representing the 25th and 75th quantiles,

the 50th quantile displayed as a line within the box, and the mean as a line extending through the box. Whiskers extend to the 10th and 90th quantiles, and circles represent outliers. Statistically significant differences were found between groups (Part B, $P<0.004$), and between the whole sperm heads upon shift in pattern (Part C, $P<0.03$), using Wilcoxon's signed rank test. The percent change in intensity was also determined for the APM, PAMP, and whole sperm head (Part D). In this part, a negative value denotes a decrease in fluorescence intensity, and a positive value an increase in fluorescence intensity.

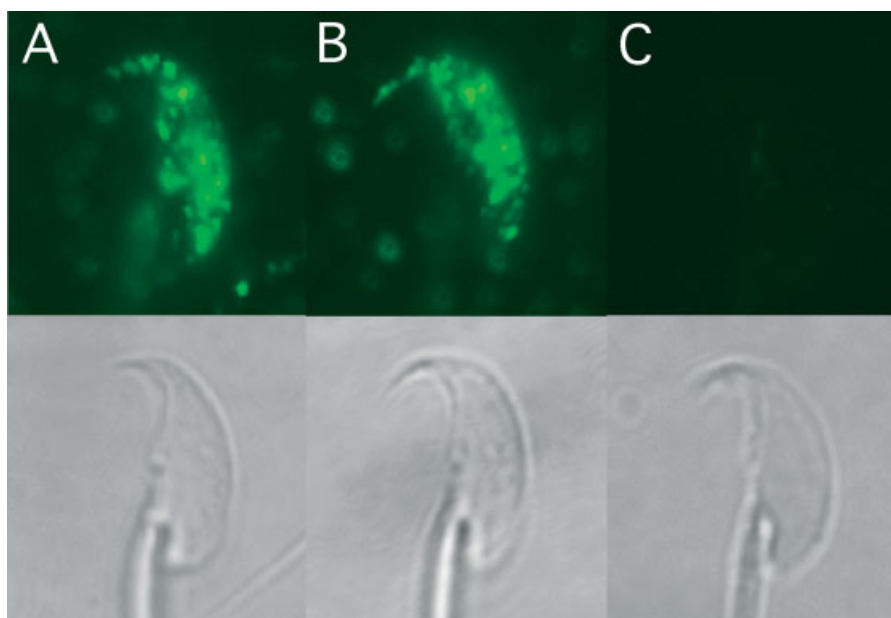


Fig. 3. Indirect immunofluorescence localization of G_{M1} in sperm fixed lightly with Fixative A. G_{M1} localization and corresponding bright field images are shown in the parts. G_{M1} localized to the APM in the heads of sperm incubated prior to fixation under both non-capacitating conditions (Part A) and after incubation with 2-OHCD (Part B) ($n=5$). A negative control performed with no primary antibody demonstrated the specificity of the secondary antibody (Part

C). In addition to the antibody not inducing redistribution to the PAMP in these lightly fixed cells, another subtle difference was also observed versus the use of CTB. With the antiserum, the fluorescence signal was patchier over the ES and AA, suggesting that crosslinking was occurring, but was different in some way versus the pentameric binding of the CTB.

TABLE 1. Patterns of G_{M1} distribution in non-capacitated sperm with different fixation conditions

Fixative	Pattern			
	APM	D	AA/PAPM	PAPM
0.004% paraformaldehyde ^a	ns	8.3 ± 2.4	16.5 ± 3.0	73.1 ± 2.4
1.25% paraformaldehyde, 2.5% glutaraldehyde, 100 mM sodium cacodylate, 0.5 mM calcium chloride ^a	75.2 ± 1.4	24.8 ± 1.4	0	0
4% paraformaldehyde, 0.1% glutaraldehyde, 5 mM calcium chloride ^a	83.7 ± 1.7	16.2 ± 1.7	0.2 ± 0.1	0

ns, not scored because this pattern had consistently less fluorescence intensity than the other patterns, and occurred in <5% of cells.

Patterns: APM, acrosomal; D, diffuse; AA/PAPM, apical acrosome and post-acrosomal; PAPM, post-acrosomal. (n = 6–15 for each fixation condition).

^aKruskal–Wallis analysis showed significant differences between patterns ($P < 0.05$).

underscore that fixation conditions can have dramatic effects on the apparent localization of lipids, and should be determined for specific cell types by work in live cells.

G_{M1} redistribution was induced by CTB

Although the data from experiments with both live and fixed sperm suggested that G_{M1} redistribution was induced by CTB in non-viable cells, a direct test was needed to show that G_{M1} redistribution was not also induced by the weak fixation conditions apart from the crosslinking by CTB. Serial fixations, first using Fixative A and then fixing the same sample with Fixative B prior to incubation with CTB, were employed to rule out this possibility. If the light fixative itself induced redistribution, then this would have resulted in the majority of the cells having a PAPM signal. However, these results showed that G_{M1} was immobilized to the APM in ~90% of the sperm (Fig. 4). This demonstrated that the redistribution of G_{M1} was due to the specific crosslinking with CTB and not induced by weak fixation. Indirect immunofluorescence on sperm fixed with Fixative A (shown previously in Fig. 3), also suggested that the specific nature of crosslinking by the pentameric CTB was critical for G_{M1} redistribution, because there can be significant crosslinking when using an indirect method with secondary antibodies, yet this did not induce redistribution. However, this variation in the nature of the crosslinking might have contributed to

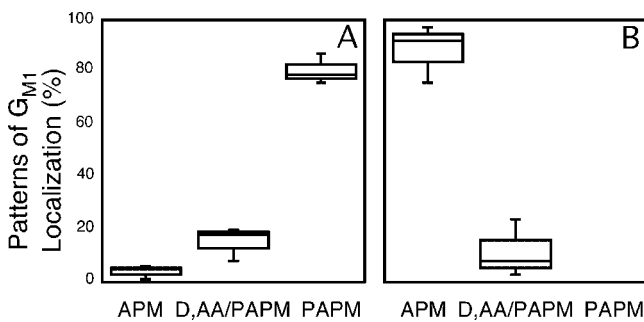


Fig. 4. Patterns of G_{M1} localization seen in sperm using weak, then strong, fixation conditions. Box plots showing percent of sperm with specific G_{M1} patterns (APM, Acrosomal; D, AA/PAPM, Diffuse or Apical Acrosomal and Post-acrosomal; PAPM, Post-acrosomal) seen with (A) incubation in Fixative A prior to incubation with CTB, and (B) serial fixation: first Fixative A, then incubating the same sample with Fixative B prior to incubation with CTB. G_{M1} distribution was predominantly seen over the PAPM with weak fixation (A); subsequent fixation of Fixative A-treated samples with Fixative B showed sperm with G_{M1} distribution predominantly over the APM (B). These data showed that the redistribution of G_{M1} to the PAPM was not induced by the weak fixation but was due to specific crosslinking by CTB.

the subtle difference in the degree of “patchiness” over the APM when using indirect immunofluorescence localization. To demonstrate further the critical role of CTB in induction of redistribution, sperm were left overnight at 37°C then assessed the next morning to verify that all were immotile. They were then fixed with Fixative B, and incubated with CTB. The vast majority of these cells displayed an APM pattern (n = 3; data not shown). This finding showed that the cessation of motility itself was not the driving force behind redistribution, but that incubation with CTB without prior heavy fixation was required for redistribution. If left at 37°C for even longer periods, the segregation of the sub-domains eventually did break down, and CTB fluorescence labeling in the sperm head took on a more diffuse pattern. By this point in time, the sperm structure and membranes showed signs of damage (data not shown).

G_{M1} redistribution was not associated with the movement of sterols

G_{M1} and sterol dual localization using CTB conjugated with Alexa Fluor 647, and filipin, respectively, was performed on sperm fixed with Fixative B (Fig. 5A,B) and Fixative A (Fig. 5C,D). With the heavy fixative, both G_{M1} (Fig. 5A) and the filipin sterol complex (Fig. 5B) localized to the APM, mirroring the localization of G_{M1} in live sperm (Fig. 1A,B), and previous reports of filipin-sterol complex localization in fixed cells. As noted above with weak fixation, G_{M1} redistributed from the APM and localized to the PAPM (Fig. 5C); however, sterols did not redistribute in these same cells (Fig. 5D). These data suggest that despite the segregation of both these “raft associated” lipids to the APM in live sperm, CTB could induce separation of G_{M1} from sterols, which maintained their original localization. When coupled with the lack of redistribution after sterol efflux, these data suggest that interactions between sterols and G_{M1} did not exclusively maintain APM sub-domain segregation.

Membrane sub-domain segregation in caveolin-1 null mice

The preferential interaction of lipids with specific proteins has been suggested to be a mechanism for the generation and maintenance of membrane sub-domains. A definitive demonstration that this model is not operative in the sperm head would require individual deletions of each membrane protein and is not practical. However, specific proteins found in sperm have been shown to interact with lipids. Of these, caveolin-1 was an attractive candidate for investigation because we have demonstrated its presence in the region of the APM (Travis et al., 2001b), and it interacts with sterols. We therefore investigated the distribution of

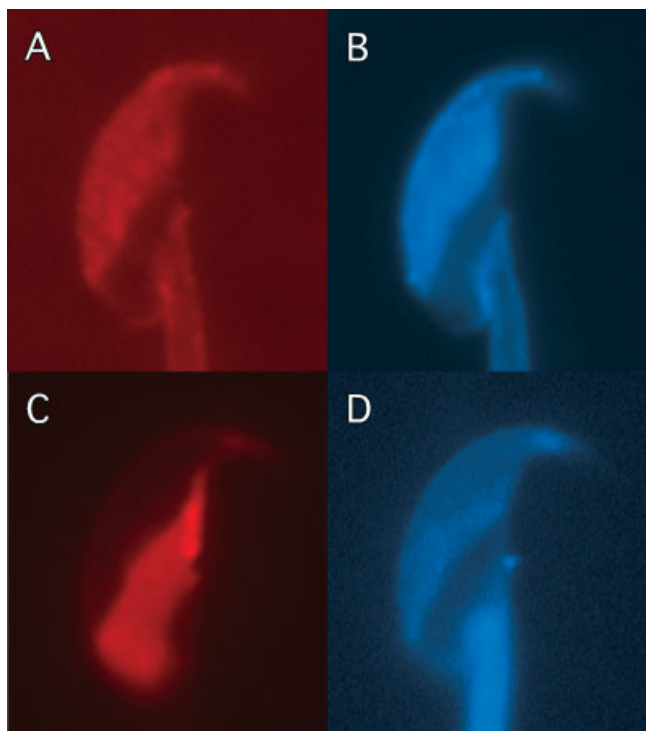


Fig. 5. Localization of G_{M1} and filipin-sterol complexes in fixed sperm. G_{M1} was localized using CTB Alexa Fluor 647 (red), and sterols were localized using filipin complex (blue) in sperm fixed with Fixative B (Parts **A** and **B**) and Fixative A (Parts **C** and **D**). With the stronger fixative, both G_{M1} (**A**) and the filipin sterol complex (**B**) localized to the APM. With weak fixation, G_{M1} redistributed from the APM (as seen in live cells; Fig. 2A) and localized to the PAPM (**C**), although sterols did not redistribute in these same cells (**D**).

G_{M1} and sterols in caveolin-1 null mice. We found both G_{M1} and sterols to be segregated to the APM (Fig. 6A,B). These data suggest that a preferential interaction between specific lipids and caveolin-1 was not needed for the maintenance of these sub-domains, and that they

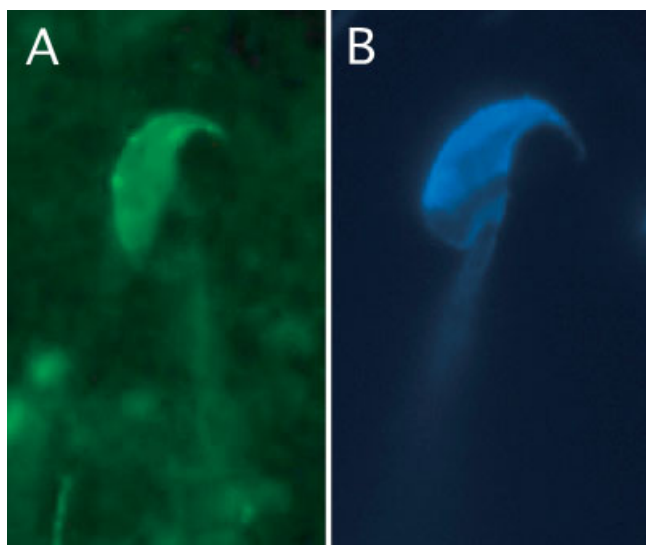


Fig. 6. Localization of G_{M1} and filipin-sterol complexes in sperm from caveolin-1^{-/-} mice. G_{M1} was localized in live sperm using CTB Alexa Fluor 488 (green, **A**), and sterols were localized using filipin complex (blue, **B**) in sperm fixed with Fixative B. Both G_{M1} and sterols localized to the APM as they did in wild-type mice of this same strain (data not shown).

could be generated in the absence of caveolin-1. Upon cessation of motility in unfixed cells or in the presence of Fixative A, G_{M1} in these caveolin-1 knock-out mice also redistributed to the PAPM (data not shown). These findings indicated that caveolin-1 was not required for the redistribution phenomenon.

Sub-domain segregation was not dependent upon ATP generation

The fact that redistribution of G_{M1} occurred at the time of cessation of motility suggested that the maintenance of sub-domain segregation might be dependent upon ATP generation. To test this possibility, we incubated sperm in the absence of metabolic substrates and in the presence of PCP and azide. After motility ceased, we treated the sperm with the strong fixative (Fixative B) to immobilize the G_{M1} as it had been prior to incubation with CTB. We found the pattern of fluorescence to be once again predominantly in the APM (data not shown). The concentration of ATP in sperm treated in this fashion was found to be at basal levels, equivalent to that seen in dead sperm left to incubate overnight in the absence of metabolic substrates, and approximately $\leq 5\%$ of that seen in live sperm (data not shown).

The membrane compartmentation model

In fixed cells, the SAR appears as a distinct ridge at the boundary between the APM and PAPM sub-domains of the sperm head when visualized by freeze fracture, atomic force microscopy, or surface replica (Friend and Fawcett, 1974; Lin and Kan, 1996; Ellis et al., 2002). A cytoskeletal barrier at this point would be consistent with the membrane compartmentation model of sub-domain segregation. In Figure 7A, SEM of unfixed, freeze-dried sperm showed that the SAR was not an artifact of fixation, but was a bona fide topographical feature. The SAR was also visible in demembranated, fixed sperm (Fig. 7B), confirming that it was an extension of the dense perinuclear theca (Olson et al., 2003), as are two of the three rods of the perforatorium (Oko and Clermont, 1988; Korley et al., 1997). Within the APM, the ES is demarcated from the AA by a groove running from the SAR to the perforatorium (Fig. 7A,B). The posterior ring delimits the lower boundary of the PAPM (Fig. 7B). These data suggested that the SAR was not an artifact of fixation or detergent, and that cytoskeletal elements delimit the APM, shown here and elsewhere to be enriched in sterols, caveolin-1 and G_{M1} (Friend, 1982; Lin and Kan, 1996; Visconti et al., 1999b; Travis et al., 2001b).

A cytoskeletal border around a membrane sub-domain is consistent with a membrane compartmentation model of segregation. To investigate potential roles for actin in this regard, we incubated sperm with cytochalasin D and latrunculin A (which sequester monomeric actin and shift the equilibrium of dynamic actin filaments to depolymerization), and swinholide A (which severs actin filaments). These agents had no effect on sub-domain segregation (Fig. 8). We next incubated sperm with acrylamide, a disruptor of intermediate filaments. Again, we saw no effect on sub-domain maintenance (Fig. 8). These agents also did not prevent the redistribution of G_{M1} to the PAPM in unfixed sperm upon the cessation of motility, or in sperm treated with the disruptors and then fixed with Fixative A ($n = 3$; data not shown).

However, when we incubated sperm with DTT, we observed an interesting effect. We saw that exposure to reducing agents prior to incubation with Fixative B

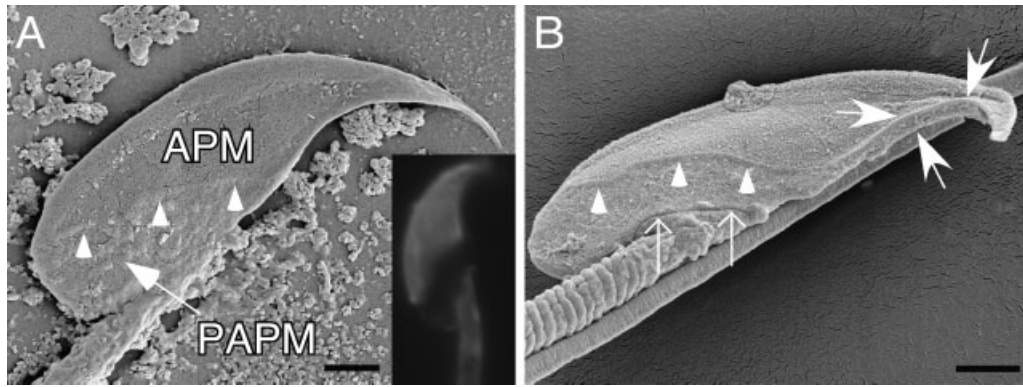


Fig. 7. Evidence of structures delineating membrane sub-domains in the sperm head. In Parts **A**, SEM of unfixed, freeze-dried sperm reveals the SAR (arrowheads) at the boundary of the APM and PAPM. The cells were neither fixed nor washed out of medium, but were freeze-dried while live in PBS, accounting for the deposits. The inset

shows the localization pattern of filipin-sterol complex in a sperm fixed with Fixative A. Part **B** shows SEM of a sperm, which lost its plasma membrane during the process of fixing/critical point drying. The SAR (arrowheads) and posterior ring (thin arrows) are noted, as are the two linear rods of the perforatorium (filled arrows).

resulted in the majority of sperm having a post-acrosomal pattern of fluorescence (Fig. 9). A similar effect was seen with β ME, although to a lesser extent (data not shown). These data implicated that disulfide bonds play an important role in the maintenance of these sub-domains. It should be noted that these effects were observed at concentrations low enough that they did not affect viability as determined by both motility and propidium iodide fluorescence (0.05 mM through 1 mM DTT; data not shown). In live cells, a small percentage of DTT-treated motile sperm also displayed a PAPM pattern of G_{M1} localization (data not shown),

suggesting both that disulfide bonds were important for the maintenance of these sub-domains, and that those proteins were either not the entire mechanism of segregation, or that the cell had some mechanism to counteract the effects of the reducing agent. Heavy fixation (Fixative B) prior to exposure to a reducing agent resulted in the maintenance of the sub-domain segregation. This finding reinforced a role for the cross-linking of specific proteins in sub-domain maintenance, as opposed to a specific role for the disulfide bonds themselves.

DISCUSSION

There have been several studies of G_{M1} localization in sperm, with results varying widely between and within species. For example, in the mouse, it has been suggested that G_{M1} localizes to the PAPM and that this localization does not change with capacitation (Trevino et al., 2001). Another study has localized G_{M1} to the midpiece and then moving to the head during capacitation (Shadan et al., 2004). These were both performed at 16°C, and phase transitions between this and physiologic temperatures (Wolf et al., 1990) might account for some disparity with our results. In rat sperm, it was suggested that G_{M1} localizes to the PAPM and then moves to the APM during capacitation (Roberts et al., 2003), whereas in human sperm, it was recently reported that G_{M1} has a diffuse localization pattern (Cross, 2004). In all of these reports, temperatures, timing of CTB treatment, the use of live, viable sperm versus different fixation conditions, and the use of epididymal versus ejaculated sperm have varied.

In this study, we observed the endogenous ganglioside G_{M1} in the plasma membrane of live murine sperm. Underscoring the difficulties inherent when studying membrane sub-domains, our data reinforce that patching artifacts dramatic in terms of size and speed of redistribution can be induced and have the potential to overcome otherwise immutable diffusion barriers, and that a given fixation condition can vary widely in its ability to immobilize membrane lipids in a given cell depending upon modulation of membrane lipids. These difficulties are likely to be found in other cell systems as well.

In living cells, we found that G_{M1} localized to the APM and segregated at the level of the SAR, matching the localization of sterols and caveolin-1 (Travis et al., 2001b) in fixed cells. Lack of movement of G_{M1} from the

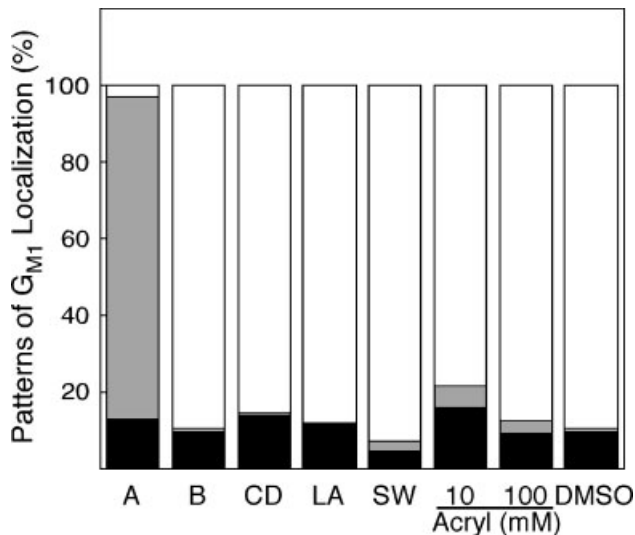


Fig. 8. Localization of G_{M1} after treatment of sperm with compounds known to disrupt the cytoskeleton. Sperm were fixed with Fixative A (**A**) or with Fixative B (**B**) as controls to induce or prevent redistribution of G_{M1} to the PAPM. Live sperm were treated with 50 μ M cytochalasin D (CD), 5 μ M latrunculin A (LA), 1 μ M swinholide (SW), two concentrations of acrylamide (Acryl) as indicated, or an equivalent volume of DMSO as a solvent control for the agents affecting actin, prior to fixation with Fixative B. In all bars, the black fill indicates the mean percentage of sperm demonstrating a diffuse pattern of G_{M1} localization, the gray fill indicates a post-acrosomal pattern, and the white fill indicates an acrosomal pattern ($n=3$ for all conditions). Statistically significant differences between conditions were noted with a Kruskal-Wallis analysis for the acrosomal pattern ($P < 0.0001$) and post-acrosomal pattern ($P < 0.0001$), whereas there was no significant difference within the diffuse pattern. No differences were apparent in pairwise comparisons between treatments with individual disruptors of the cytoskeleton and the heavy Fixative (bar B).

APM to the PAPM, even over periods of hours, argued against a “transient confinement zone” model of sub-domain segregation. Within 10–100 sec of the cessation of motility, the CTB fluorescence redistributed dramatically, decreasing in the APM and intensifying in the PAPM. The timing of this change suggested that in a live cell, the mechanism of segregation functioned to resist the perturbation energy imparted by the crosslinking CTB. At the time of cessation of motility/cell death, that mechanism was compromised in some way such that the crosslinked G_{M1} was induced to move across the SAR. Interestingly, ATP was not required for maintenance of segregation. This was not unexpected given the lack of ATP-generating pathways in the sperm head [Please see (Travis and Kopf, 2002) for a review.].

Sterols visualized with filipin in the APM were stably segregated even after the redistribution of G_{M1} to the PAPM. This finding suggests that even though sterols and G_{M1} co-localized in the APM and were segregated at the same boundary of the SAR, the mechanisms that maintain segregation of these two lipids could be different or that the lipids are separable. In either case, both this finding and the fact that sterol efflux did not

facilitate movement of G_{M1} across the SAR, suggest that interactions between sterols and G_{M1} do not maintain sub-domain segregation. Whether the co-localized G_{M1} , sterols, and caveolin-1 are all members of an integrated, single APM raft, or are components of numerous small-scale heterogeneities within the APM, awaits further investigation.

Although segregation of sterol-rich and sterol-poor membrane sub-domains has been noted in fixed sperm at the SAR boundary, results from protein and lipid localization experiments, including fluorescence recovery after photobleaching in live sperm, often disagree regarding the ability of the SAR or other potential “fences” (e.g., posterior ring and annulus) to act as barriers to lateral diffusion. For example, some proteins and lipid probes have been shown to be restricted to specific membrane domains (Myles et al., 1984; Phelps et al., 1988; Friend, 1989; Nehme et al., 1993), but others have been demonstrated to diffuse freely across the cytoskeletal structures underlying these putative barriers (Wolfe et al., 1998; Mackie et al., 2001; Christova et al., 2004). Apart from methodology, one explanation for these differences might be that the barriers are effective primarily against endogenous membrane constituents. This would imply either defined interactions between membrane molecules and the “fence”, or interactions between membrane constituents with underlying structures (i.e., “anchors”). Exogenous probes might behave anomalously, moving between the anchored native molecules or penetrating the fence to varying degrees.

Either a lipid shell or membrane compartmentation model would be consistent with these kinds of variations in data observed with exogenous probes, and could be consistent with the structures underlying a proposed barrier to lateral diffusion at the SAR. As noted, it is impossible to rule out the lipid shell model definitively, but we did observe that the absence of the sterol-binding protein, caveolin-1, did not affect the segregation of G_{M1} or sterols. We hypothesized that the “fence” of the SAR

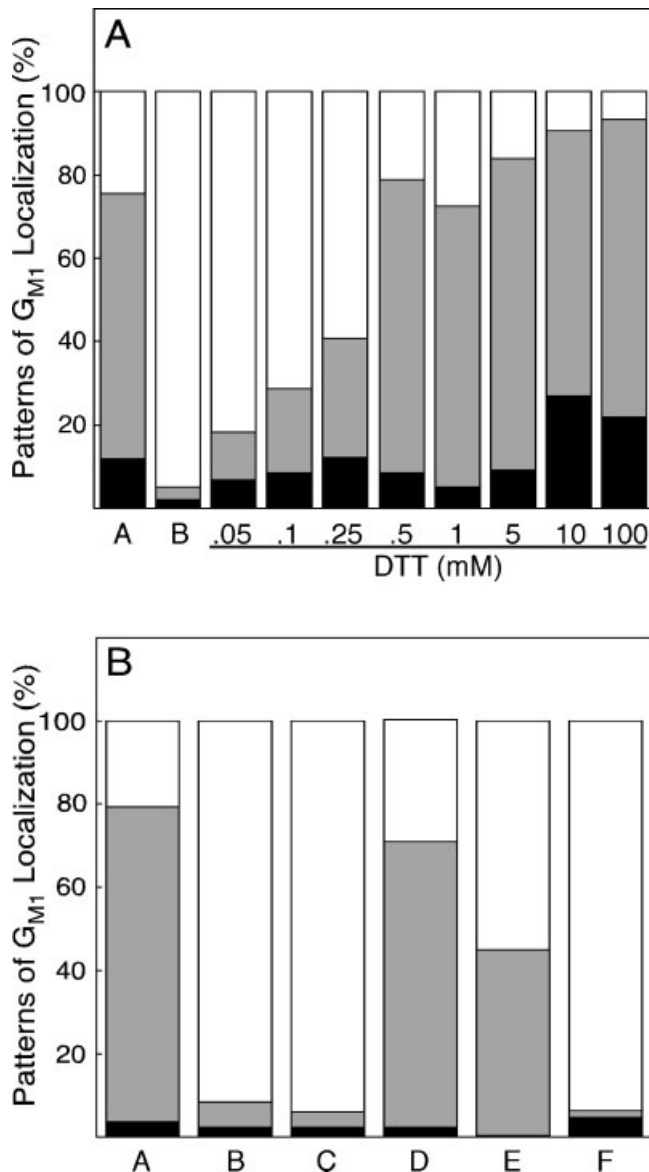


Fig. 9. Localization of G_{M1} after treatment of sperm with disulfide-reducing agents. Part A: Sperm were fixed with Fixative A (bar A) or with Fixative B (bar B) as controls to induce or prevent redistribution of G_{M1} to the PAPM. Live sperm were treated with varying concentrations of DTT as indicated. After treatment with DTT, the sperm were incubated with Fixative B, and G_{M1} was localized using CTB. In all bars, the black fill indicates the mean percentage of sperm demonstrating a diffuse pattern of G_{M1} localization, the gray fill indicates a post-acrosomal pattern, and the white fill indicates an acrosomal pattern ($n = 3$ for all conditions). Statistically significant differences between conditions were noted with a Kruskal–Wallis analysis for the acrosomal pattern ($P < 0.002$) and post-acrosomal pattern ($P < 0.004$), whereas there was no significant difference within the diffuse pattern. Concentrations of DTT ≥ 0.1 mM were significantly different regarding the acrosomal and post-acrosomal patterns in pairwise comparisons with the heavy fixative (bar B) ($P < 0.025$ for all comparisons). Part B: Bars A and B were fixed as in Part A. In bar C, sperm were fixed first in Fixative A and then with Fixative B. In bar D, sperm were treated while live with 1 mM DTT and then fixed in Fixative B. In bar E, sperm were fixed first in Fixative A, then treated with 1 mM DTT, and then fixed with Fixative B, whereas in bar F, the sperm were fixed first with Fixative B then treated with DTT. The shades of fill represent the same patterns of localization as in Part A ($n = 5$ for all conditions). Statistically significant differences between conditions were noted with a Kruskal–Wallis analysis for the acrosomal pattern ($P < 0.0001$) and post-acrosomal pattern ($P < 0.0001$), whereas there was no significant difference within the diffuse pattern. Pairwise comparisons between treatment conditions showed no significant differences between bars B, C, and F for the acrosomal and post-acrosomal patterns. These results show that fixation alone did not induce a change in pattern of G_{M1} localization, and that heavy fixation (Fixative B) prior to treatment with DTT prevented redistribution (bar F), whereas light fixation (Fixative A) only moderately weakened the effect of DTT.

would likely be composed of cytoskeletal proteins such as actin and/or vimentin, both of which help comprise larger structures such as the perinuclear theca and perforatorium (Virtanen et al., 1984; Oko et al., 1990; Breed et al., 2000), and associate with lipid-binding proteins such as PERF-15 (Oko and Morales, 1994; Schmitt et al., 1994). However, it is not surprising that dynamic actin filaments are not involved in the segregation (as indicated by the data from cytochalasin D and latrunculin A treatments), due to the facts that sperm must be kept in a quiescent state while stored in the epididymis, and do not have ATP-generating pathways in the sperm head. The finding that disulfide bonds between proteins are essential for sub-domain segregation is intriguing. Given that sperm have minimal cytoplasm underlying the plasma membrane, this membrane could interact intimately with structures such as the SAR and perforatorium. These structures arise from the perinuclear theca, and have components attached to them via disulfide bonds (Perry et al., 1999); however, the perinuclear theca is itself not solubilized by treatment with disulfide-reducing agents (Sutovsky et al., 1997). We are now investigating the proteome of these structures to identify the critical proteins and interactions involved.

The question arises as to why sperm possess such large, stable membrane sub-domains when compared with other cells. Several possible functions are consistent with the data: (1) a rigid/highly ordered APM might prevent premature fusion with the outer acrosomal membrane, perhaps by decreasing permeability to Ca^{++} , a trigger of acrosomal exocytosis, (2) sterol efflux from an ordered APM to oviductal HDL and albumin (Langlais et al., 1988; Ehrenwald et al., 1990) could provide a "sensing mechanism" so that capacitation occurs in the oviduct, (3) a single, large membrane sub-domain might help target protein machinery needed to interact with the egg, and (4), differences in APM raft composition might define sub-populations of sperm capable of capacitating at different times, expanding the window of opportunity to fertilize eggs (Flesch et al., 2001).

The localization and movement of G_{M1} in murine sperm is remarkable for several reasons. First, it provides evidence in living cells for the existence of membrane sub-domains, still a matter of some controversy (Munro, 2003). Second, it shows that these sub-domains can exist on a micron scale and over a long time period in viable cells. The large size of these sub-domains makes sperm an ideal model system for the study of sub-domain segregation, in particular when compared with the types of sub-domains more typical of somatic cells. Finally, understanding of these sub-domains sheds important light on understanding the nature of sperm capacitation, such as how stimuli like sterol efflux can be transduced into the functional changes that allow a sperm to fertilize an egg.

ACKNOWLEDGMENTS

We thank Dr. Hollis Erb (Cornell University) for her help with statistical analysis and Carole Daugherty at the Cornell Integrated Microscopy Center for performing the SEM. The study was supported by National Institutes of Health; contract grant numbers: K01-RR00188 and R01-HD-045664 (A.J.T.); P01-HD-06274 (Stuart B. Moss, Carmen J. Williams, and G.S.K.); R01-CA-98779 and R01-CA-80250 (M.P.L.); T32-GM07288 (A.W.C.); Dual Degree Program of the Cornell University College of Veterinary Medicine (D.E.B.); American

Heart Association Established Investigator Award; contract grant number: 0540113N (M.P.L.); Hirschl/Weil-Caulier Career Scientist Award (M.P.L.).

LITERATURE CITED

- Breed WG, Idriss D, Oko RJ. 2000. Protein composition of the ventral processes on the sperm head of Australian hydromyine rodents. *Biol Reprod* 63(2):629–634.
- Christova Y, James P, Mackie A, Cooper TG, Jones R. 2004. Molecular diffusion in sperm plasma membranes during epididymal maturation. *Mol Cell Endocrinol* 216(1–2):41–46.
- Clark JM, Koehler JK. 1990. Observations of hamster sperm-egg fusion in freeze-fracture replicas including the use of filipin as a sterol marker. *Mol Reprod Dev* 27(4):351–365.
- Cross NL. 2004. Reorganization of lipid rafts during capacitation of human sperm. *Biol Reprod* 71(4):1367–1373.
- Davis BK. 1976. Influence of serum albumin on the fertilizing ability in vitro of rat spermatozoa. *Proc Soc Exp Biol Med* 151(2):240–243.
- Ehrenwald E, Foote RH, Parks JE. 1990. Bovine oviductal fluid components and their potential role in sperm cholesterol efflux. *Mol Reprod Dev* 25:195–204.
- Ellis DJ, Shadan S, James PS, Henderson RM, Michael Edwardson JM, Hutchings A, Jones R. 2002. Post-testicular development of a novel membrane substructure within the equatorial segment of ram, bull, boar, and goat spermatozoa as viewed by atomic force microscopy. *J Struct Biol* 138(3):187–198.
- Flesch FM, Brouwers JF, Nievelstein PF, Verkleij AJ, van Golde LM, Colenbrander B, Gadella BM. 2001. Bicarbonate stimulated phospholipid scrambling induces cholesterol redistribution and enables cholesterol depletion in the sperm plasma membrane. *J Cell Sci* 114(Pt 19):3543–3555.
- Friend DS. 1982. Plasma-membrane diversity in a highly polarized cell. *J Cell Biol* 93(2):243–249.
- Friend DS. 1989. Sperm maturation: Membrane domain boundaries. *Ann NY Acad Sci* 567:208–221.
- Friend DS, Fawcett DW. 1974. Membrane differentiations in freeze-fractured mammalian sperm. *J Cell Biol* 63(2 Pt 1):641–664.
- Gaus K, Gratton E, Kable EP, Jones AS, Gelissen I, Kritharides L, Jessup W. 2003. Visualizing lipid structure and raft domains in living cells with two-photon microscopy. *Proc Natl Acad Sci USA* 100(26):15554–15559.
- Harrison RA, Vickers SE. 1990. Use of fluorescent probes to assess membrane integrity in mammalian spermatozoa. *J Reprod Fertil* 88(1):343–352.
- Kim KS, Gerton GL. 2003. Differential release of soluble and matrix components: Evidence for intermediate states of secretion during spontaneous acrosomal exocytosis in mouse sperm. *Dev Biol* 264(1):141–152.
- Korley R, Poursmaeili F, Oko R. 1997. Analysis of the protein composition of the mouse sperm perinuclear theca and characterization of its major protein constituent. *Biol Reprod* 57(6):1426–1432.
- Kusumi A, Koyama-Honda I, Suzuki K. 2004. Molecular dynamics and interactions for creation of stimulation-induced stabilized rafts from small unstable steady-state rafts. *Traffic* 5(4):213–230.
- Langlais J, Kan FWK, Granger L, Raymond L, Bleau G, Roberts KD. 1988. Identification of sterol acceptors that stimulate cholesterol efflux from human spermatozoa during in vitro capacitation. *Gamete Res* 20:185–201.
- Lauer S, Goldstein B, Nolan RL, Nolan JP. 2002. Analysis of cholera toxin-ganglioside interactions by flow cytometry. *Biochem* 41(6):1742–1751.
- Lin Y, Kan FW. 1996. Regionalization and redistribution of membrane phospholipids and cholesterol in mouse spermatozoa during in vitro capacitation. *Biol Reprod* 55(5):1133–1146.
- Mackie AR, James PS, Ladha S, Jones R. 2001. Diffusion barriers in ram and boar sperm plasma membranes: Directionality of lipid diffusion across the posterior ring. *Biol Reprod* 64(1):113–119.
- Maxfield FR. 1982. Weak bases and ionophores rapidly and reversibly raise the pH of endocytic vesicles in cultured mouse fibroblasts. *J Cell Biol* 95(2 Pt 1):676–681.
- Munro S. 2003. Lipid rafts: Elusive or illusive? *Cell* 115(4):377–388.
- Myles DG, Primakoff P, Koppel DE. 1984. A localized surface protein of guinea pig sperm exhibits free diffusion in its domain. *J Cell Biol* 98(5):1905–1909.
- Nehme CL, Cesario MM, Myles DG, Koppel DE, Bartles JR. 1993. Breaching the diffusion barrier that compartmentalizes the transmembrane glycoprotein CE9 to the posterior-tail plasma membrane domain of the rat spermatozoon. *J Cell Biol* 120:687–694.
- Oko R, Clermont Y. 1988. Isolation, structure and protein composition of the perforatorium of rat spermatozoa. *Biol Reprod* 39(3):673–687.
- Oko R, Morales CR. 1994. A novel testicular protein, with sequence similarities to a family of lipid binding proteins, is a major component of the rat sperm perinuclear theca. *Dev Biol* 166:235–245.
- Oko R, Moussakova L, Clermont Y. 1990. Regional differences in composition of the perforatorium and outer periacrosomal layer of the rat spermatozoon as revealed by immunocytochemistry. *Am J Anat* 188(1):64–73.
- Olson GE, Winfrey VP, Nagdas SK. 2003. Structural modification of the hamster sperm acrosome during posttesticular development in the epididymis. *Microsc Res Tech* 61(1):46–55.
- Pelletier RM, Friend DS. 1983. Development of membrane differentiations in the guinea pig spermatid during spermiogenesis. *Am J Anat* 167(1):119–141.
- Perry AC, Wakayama T, Yanagimachi R. 1999. A novel trans-complementation assay suggests full mammalian oocyte activation is coordinately initiated by multiple, submembrane sperm components. *Biol Reprod* 60:747–755.
- Phelps BM, Primakoff P, Koppel DE, Low MG, Myles DG. 1988. Restricted lateral diffusion of PH-20, a PI-anchored sperm membrane protein. *Science* 240:1780–1782.
- Razani B, Engelman JA, Wang XB, Schubert Z, Zhou XL, Marks CB, Macaluso F, Russell RG, Li M, Pestell RG, Di Vizio D, Hou H, Jr., Knietz B, Lagaud G, Christ GJ, Edelmann W, Lisanti MP. 2001. Caveolin-1 null mice are viable, but show evidence of hyper-proliferative and vascular abnormalities. *J Biol Chem* 276:1616.
- Roberts KP, Wamstad JA, Ensrud KM, Hamilton DW. 2003. Inhibition of capacitation-associated tyrosine phosphorylation signaling in rat sperm by epididymal protein Crisp-1. *Biol Reprod* 69(2):572–581.

- Schmitt MC, Jamison RS, Orgebin-Crist MC, Ong DE. 1994. A novel, testis-specific member of the cellular lipophilic transport protein superfamily, deduced from a complimentary deoxyribonucleic acid clone. *Biol Reprod* 51(2):239–245.
- Shadan S, James PS, Howes EA, Jones R. 2004. Cholesterol Efflux Alters Lipid Raft Stability and Distribution During Capacitation of Boar Spermatozoa. *Biol Reprod* 71:253–265.
- Simons K, Toomre D. 2000. Lipid rafts and signal transduction. *Nat Rev Mol Cell Biol* 1:31–39.
- Sutovsky P, Oko R, Hewitson L, Schatten G. 1997. The removal of the sperm perinuclear theca and its association with the bovine oocyte surface during fertilization. *Dev Biol* 188(1):75–84.
- Suzuki F. 1988. Changes in the distribution of intramembranous particles and filipin-sterol complexes during epididymal maturation of golden hamster spermatozoa. *J Ultrastruct Mol Struct Res* 100(1):39–54.
- Travis AJ, Kopf GS. 2002. The spermatozoon as a machine: Compartmentalized pathways bridge cellular structure and function. In: De Jonge CJ, Barratt CL, editors. *Assisted reproductive technology: Accomplishments and new horizons*. Cambridge: Cambridge University Press. pp 26–39.
- Travis AJ, Jorgez CJ, Merdiushev T, Jones BH, Dess DM, Diaz-Cueto L, Storey BT, Kopf GS, Moss SB. 2001a. Functional relationships between capacitation-dependent cell signaling and compartmentalized metabolic pathways in murine spermatozoa. *J Biol Chem* 276:7630–7636.
- Travis AJ, Merdiushev T, Vargas LA, Jones BH, Purdon MA, Nipper RW, Galatioto J, Moss SB, Hunnicutt GR, Kopf GS. 2001b. Expression and localization of caveolin-1, and the presence of membrane rafts, in mouse and Guinea pig spermatozoa. *Dev Biol* 240(2):599–610.
- Trevino CL, Serrano CJ, Beltran C, Felix R, Darszon A. 2001. Identification of mouse trp homologs and lipid rafts from spermatogenic cells and sperm. *FEBS Lett* 509(1):119–125.
- Virtanen I, Badley RA, Paasivuo R, Lehto VP. 1984. Distinct cytoskeletal domains revealed in sperm cells. *J Cell Biol* 99(3):1083–1091.
- Visconti PE, Galantino-Homer H, Ning X, Moore GD, Valenzuela JP, Jorgez CJ, Alvarez JG, Kopf GS. 1999a. Cholesterol efflux-mediated signal transduction in mammalian sperm. b-cyclodextrins initiate transmembrane signaling leading to an increase in protein tyrosine phosphorylation and capacitation. *J Biol Chem* 274:3235–3242.
- Visconti PE, Ning X, Fornes MW, Alvarez JG, Stein P, Connors SA, Kopf GS. 1999b. Cholesterol efflux-mediated signal transduction in mammalian sperm: Cholesterol release signals an increase in protein tyrosine phosphorylation during mouse sperm capacitation. *Dev Biol* 214(2):429–443.
- Wolf DE, Maynard VM, McKinnon CA, Melchior DL. 1990. Lipid domains in the ram sperm plasma membrane demonstrated by differential scanning calorimetry. *Proc Natl Acad Sci USA* 87(17):6893–6896.
- Wolfe CA, James PS, Mackie AR, Ladha S, Jones R. 1998. Regionalized lipid diffusion in the plasma membrane of mammalian spermatozoa. *Biol Reprod* 59(6):1506–1514.
- Zacharias DA, Violin JD, Newton AC, Tsien RY. 2002. Partitioning of lipid-modified monomeric GFPs into membrane microdomains of live cells. *Science* 296(5569):913–916.